Arabian Journal of Chemistry (2022) **15**, 103710

King Saud University

Arabian Journal of Chemistry

www.ksu.edu.sa
www.sciencedirect.com

ORIGINAL ARTICLE

Development of [(2*E*,6*E*)-2,6-bis(4-(dimethylamino) benzylidene)cyclohexanone] as fluorescence-on probe for Hg^{2+} ion detection: Computational aided experimental studies

Jehangir Khan [a], Maria Sadia [a,*], Syed Wadood Ali Shah [b], Muhammad Zahoor [c,*], Khalaf F Alsharif [d], Fakhria A. Al-Joufi [e]

[a] *Department of Chemistry, University of Malakand, Chakdara, Lower Dir 18800, Khyber Pakhtunkhwa, Pakistan*
[b] *Department of Pharmacy, University of Malakand, Chakdara, Lower Dir 18800, Khyber Pakhtunkhwa, Pakistan*
[c] *Department of Biochemistry, University of Malakand, Chakdara, Lower Dir 18800, Khyber Pakhtunkhwa, Pakistan*
[d] *Department of Clinical Laboratory Sciences, College of Applied Medical Sciences, Taif University, P.O. Box 11099, Taif 21944, Saudi Arabia*
[e] *DepartmentofPharmacology, College of Pharmacy, Jouf University, 72341 Aljouf, Saudi Arabia*

Received 1 December 2021; accepted 16 January 2022
Available online 20 January 2022

KEYWORDS

Real time analysis;
Fluorescence-on;
Aqueous sample;
Curcumin derivative;
Hg^{2+} ion

Abstract Selective metal ion detection is highly desired in fluorometric analysis. In the current study a curcumin-based fluorescence-on probe/[(2*E*,6*E*)-2,6-bis(4-(dimethylamino) benzylidene) cyclohexanone]/probe was designed for the removal of one of the most toxic heavy metal ion i.e. Hg^{2+}. The structure of the probe was confirmed by FTIR and ^1H NMR spectroscopic analysis displaying distinctive peaks. The complex formation between probe and Hg^{2+} ion was also studied by density functional theory to support the experimental results. Chelation enhanced fluorescence was observed upon interaction with Hg^{2+} ion. Different parameters like pH, effect of mercury ion concentration, contact time, interference study and effect of probe concentration on the fluorescence enhancement were also investigated. A rapid response was detected for Hg^{2+} ion with limit of detection and quantification as 2.7 nM and 3 nM respectively with association constant of

* Corresponding authors.
E-mail addresses: mariasadia@gmail.com (M. Sadia), mohammadzahoorus@yahoo.com (M. Zahoor), alsharif@tu.edu.sa (K.F Alsharif), aaljoufi@ju.edu.sa (F.A. Al-Joufi).
Peer review under responsibility of King Saud University.

Production and hosting by Elsevier

https://doi.org/10.1016/j.arabjc.2022.103710

1×10^{11} M^{-2}. The probe displayed maximum fluorescence intensity at physiological pH. The results showed that the synthesized probe can be employed as an excellent probe for the detection and quantification of Hg^{2+} ions in aqueous samples with high selectivity and sensitivity due to its higher binding energy and larger charge transferring ability.

1. Introduction

Due to the rapid urbanization and industrialization, water crisis has become a serious problem for all forms of life on earth, from microorganisms to humans (Idros and Chu, 2018). Monitoring of the contaminants in water is of particular importance to ensure the quality of surface, ground, and drinking water. Among the several water pollutants, heavy metal ions, specifically mercury ion, is crucial for its high toxicity (Razavi et al., 2017, Hakimifar and Morsali, 2018). In recent years, mercury ion contamination in the aquatic environment has attracted global attention; therefore, the development of fluorescence based probe for Hg^{2+} ion detection is highly desired (Zhao et al., 2017). Mercury contamination of water bodies is either from natural or man-made activities. The natural sources of water contamination include rock weathering and geological matrix erosion, resulting in metal incorporation (Sunet al., 2018). Anthropogenic contamination occur through a number of means like burning of fossil fuel, metallurgy, transport sector, disposal of untreated effluents, fertilizers, pesticides in agricultural fields, discharge of industrial wastes, and leaching of metal ions into water due to acid rain (Heet al., 2018, Van et al., 2018). It is ubiquitous in the environment and is inevitable for both humans and animals being persistent environmental contaminants and cannot easily be degraded (Joksimovic and Stankovic, 2012). Organic form of mercury ion as well as inorganic form is toxic for organisms. Moreover, it exhibits bio-magnification in aquatic food chains. The mercury content of food is highly variable depending upon the nature of product, its origin and industrial processes (Streets et al., 2017). Mercury being a unique heavy metal exists in different forms i.e Hg^{2+}, Hg°, and methyl-Hg. In soil the ionic form (Hg^{2+}) is predominantly present. When mercury ion enters into organisms' bodies through water, bio-accumulation occurs over a period of time (Gonzalez et al., 2017). Mercury ion also crosses the blood–brain barrier and exhibit long-term retention thereby accumulate in vital organs of organisms, causing severe effects in liver and kidney including development of autoimmunity, reduced growth, organ damage, cancer, nervous system disorders and even death (Gonzalez et al., 2017).

Different methods have been developed for trace level detection of mercury ion in aqueous samples including liquid–liquid extraction (Panhwar et al., 2017), co-precipitation (Richard et al., 2016), resin chelation (Maet al, 2011), electrochemical deposition (Dinget al., 2014), solid phase extraction (Date et al., 2013), atomic absorption spectroscopy (Agheriand and Naderi 2009), inductively coupled plasma mass spectrometry (Louieet al., 2012) and polarography (Somersetet al., 2011); all of them involve complicated instrumentation and require sample treatment, therefore their applications are limited (Novaaket al., 2016). The electroanalytical methods and potentiometric methods are also used for biological and environmental analysis but potentiometric methods show rapid response with higher sensitivity and precision as compared to electrochemical methods (JG, M. 2017, Manjunatha, J. G. 2018, Manjunathaa, J. G et al., 2014). Fluorescence based detection of contaminants is highly demanded now a days because of their high sensitivity, multiple sensing parameters, non-destructive nature, high specificity, portability, fast response time, technical simplicity, and real-time determination of analyte. For this purpose, various optical probes have been developed. Among the optical probes, fluorescence-based detection of mercury ion has been proved to be advantageous over other methods (Ullah et al., 2018). Fluorescence-based small organic molecules for mercury ion detection have already been reported; however, they show limited application due to quenching of fluorescence caused by mercury ion coordination (Chenet al., 2011). Curcumin derivatives can be employed as a fluorescence-on probes for metal ions detection in water samples in addition to being a potential drug molecule (Hoet al., 2011). Curcumin based probes possess keto-enol tautomer due to the availability of conjugated moiety. The tautomeric forms further be classified into their *cis* and *trans* isomers. All of these isomers of conjugated carbon chain contribute to the complex behavior of curcumin. On the basis of their absorption analysis and fluorescence based detection; they provide potential applications to various environmental samples (Linet al., 2017).

Several ligands/probes with different moieties have already been developed for metal ions detection. However, the development of a cheap, and facile synthetic approach toward selective Hg^{2+} ion detection remains a hot research area. Therefore, in the current study, we aimed to design and synthesize curcumin derivative as a fluorescence-on probe for selective detection of Hg^{2+} ion in water samples. In the current study, the probe has been employed for real time detection of trace level of mercury ions at physiological pH in aqueous samples but the probe has also potency to be used as an antioxidant and anti-inflammatory agent and has role in enzyme inhibition as well. The method used in the current study is cheap, sensitive, and environmentally friendly and can easily be performed with prominent results. A comparison of the current work with the already reported work has been given in Table 1. The current method involving the synthesized fluorescent on probe shows higher limit of detection and quantification in nM range and higher association constant as compared to reported methods with real time detection of mercury ions at physiological pH.

2. Experimental methodologies

2.1. Chemicals and instruments

Cyclohexanone, 4-dimethyl aminobenaldehyde, NaOH (sigma Aldrich), all metal salts, in the form of chloride or nitrate including $Cd(NO_3)_2{\cdot}4H_2O$, $Hg(NO_3)_2$, $Ca(NO_3)_2{\cdot}4H_2O$, $Ce(NO_3)_3{\cdot}6H_2O$, $FeCl_2$, $AlCl_3{\cdot}6H_2O$, $MgCl_2{\cdot}4H_2O$, $Zn(NO_3)_2{\cdot}6H_2O$, $CuCl_2{\cdot}2H_2O$, $Mn(NO_3)_2{\cdot}4H_2O$, $Cr(NO_3)_3$, $Fe(NO)_3{\cdot}9H_2O$, $Pb(NO_3)_3$ and $NiCl_2{\cdot}6H_2O$, were purchased from Merck and used without any purification. All the fluorescence and absorption analysis were performed with a spectrophotofluorometer RF-5301 PC (Shimadzu, Japan and 1601 Double-beam UV–Visible Spectrophotometer (Kyoto, Japan). ^{1}H NMR and FTIR spectra were recorded on a Bruker Avance 400 MHz spectrometer (Varian) and FTIR instrument Pretige 21 (Shimadzu, Japan) in 400–4000 cm^{-1} range respectively. All chemical shifts were recorded on the δ-scale in deuterated chloroform ($CDCl_3$) solvent. Measurements of pH were done using a digital pH meter (Merck). All the graphs and data analysis were performed on Origin pro-8.5.

2.2. Synthesis and characterization

The probe/[(2*E*,6*E*)-2,6-bis(4-(dimethylamino)benzylidene)cyclohexanone] was synthesized by adopting the previously

Table 1 Comparison of current research work with already published work in literature.

Reagent	LOD (M)	Association constant (M^{-2})	Detection mode	Sample	Ref.
1,7-bis[4′-bromo-butaneyloxy-3′ -methyloxy-phenyl]-1,6-heptadiene-3,5-dione					
	2.54×10^{-6}	2.52×10^{4}	fluorescence-on	water	(Xu et al., 2016)
curcumin-loaded cellulose acetate	20×10^{-6}	4.23×10^{7}	fluorescence-off	water	(Raj and Shankaran, 2016)
Curcumin immobilized zeolitic imidazolate	7.64×10^{-6}	1×10^{13}	turn off fluorescence	water	(Kumar et al., 2021)
Curcumin	5×10^{-6}	NA	fluorescence-on	water	(Liu et al., 2017)
gold nanoparticles	4.0×10^{-10}	NA	fluorescence-on	water	(Zheng et al., 2009)
Probe	2.7 nM	1×10^{11}	fluorescence-on	Natural water	**Current work**

reported procedure (Zhiquan et al., 2013, Meenatchi et al., 2015, Wijianto et al., 2020). For the preparation of probe, the reagents cyclohexnone 0.12 g (5 mmol) and 4-dimethylaminobenzaldehyde 0.23 g (10 mmol) were dissolved in 20 mL absolute ethanol. The mixture was stirred for 5 min and, cooled to 0 °C (ice bath) prior to the addition of 10 mL of 10 % sodium hydroxide aqueous solution in drop wise manner. The mixture was refluxed under vigorous magnetic stirring for 3 h and the reaction progress was monitored through TLC, using ethyl acetate, *n*-hexane mixture in 1:4 ratio respectively, as the solvent system (Liu et al., 2013). After completion of reaction at 0 °C, to neutralize the reaction 30 % HCl aqueous solution was used. The precipitates of the product formed were filtered and dried under reduced pressure. (Scheme1) presents the detailed mechanism of probe. The final product was recrystallized from chloroform and yellow crystals, mp135 °C, yield 78 %. The IR (KBr) spectrum of the probe (ν cm^{-1}): 1620–1640 (C = C Ar), 2920–2835 (C-H asymmetric), 1296, (C-N) 1689 (C = O) 3028, (C-H Ar) (Fig.S1) (Swayamsiddha et al., 2019). ^{1}H NMR spectrum of the probe δH (400 MHz, $CDCl_3$), 3.103 (s, 12H, 2 × N $(CH_3)_2$), 6.69–6.73 (4H, ph), 7.41–7.70 (4H, ph), 7.403–7.562 (2H, ph) (Fig. S2) (Badal et al., 2020).

2.3. Computational details

All the Computational calculations were carried out using density functional theory (DFT) Becke's Lee-Yang-Parr's correlation function (B3LYP) (Nehla et al., 2019) Gaussian-09 code (Marenich et al., 2011).The Empirical Dispersion = GD3 (Grimme, 2006) was used to accurately describe correction in the intermolecular interactions during the complexation. The 6-31G(d,p) basis set was used for all nonmetals elements like H, C, N and O while LANL2DZ basis set was used for Hg^{2+} ion. The frequency calculations were employed to ensure whether, the geometries correspond to potential energy minima or not as well to compute the thermodynamic parameters. The imaginary frequency absence confirmed that all the geometries correspond to potential energy minima. The contribution of electrostatic effects to the binding energies and thermodynamic data were computed by employing the conductor-like polarizable continuum model (CPCM) (Marenich et al., 2009, Arakaki et al., 2013). To evaluate the binding energy (E_{bind}), Eq. (1) was used;

$$E_{bind=}E_{complex}-(E_{probe}+Hg^{2+}) \quad (1)$$

Where, $E_{complex}$ is the total energy of the complex (probe and mercury ion) while E_{probe} and E_{Hg}^{2+} are the total energy of the (probe) and Hg^{2+} ion separately. The change in enthalpy (ΔH) and Gibbs free energy (ΔG) are calculated using Eqs. (2) and (3) respectively;

$$\Delta H_{bind=}H_{complex} - H_{(probe+Hg2+)} \quad (2)$$

$$\Delta G_{bind=}\Delta H_{bind} - T\Delta S_{bind} \quad (3)$$

$$\Delta H_{bind} - T(S + S_{(probe+Hg2+)})$$

Where, "H" represents the sum of electronic and thermal enthalpy, "G" is the sum of electronic and thermal Gibbs free energy and "S" is the entropy at 298.15 K and 1 atm.

2.4. Spectroscopic studies

UV–Visible and fluorescence spectroscopy were used for exploring the optical properties and sensing ability of metal ions. In all experiments probe was prepared in pure acetonitrile and metal ion solutions (stock and working) were prepared in distilled water. The complex between probe and Hg^{2+} was prepared in mixture of acetonitrile and water in 3:2 ratio. The UV–Visible spectra of probe (6 μM) alone in acetonitrile and its complex with Hg^{2+} ion (15 μM) were taken. Similarly, the fluorescence response of probe at pH 7 was measured separately for probe and its complex with metal ions in aqueous samples. The probe-metal ion mixtures were equilibrated at room temperature before measuring the fluorescence response.

2.5. Fluorogenic recognition of Hg^{2+} ion in spiked water samples

The efficacy of probe towards Hg^{2+} ion detection was evaluated in different spiked water samples. For this purpose, lake water, river water and tap water samples were collected from

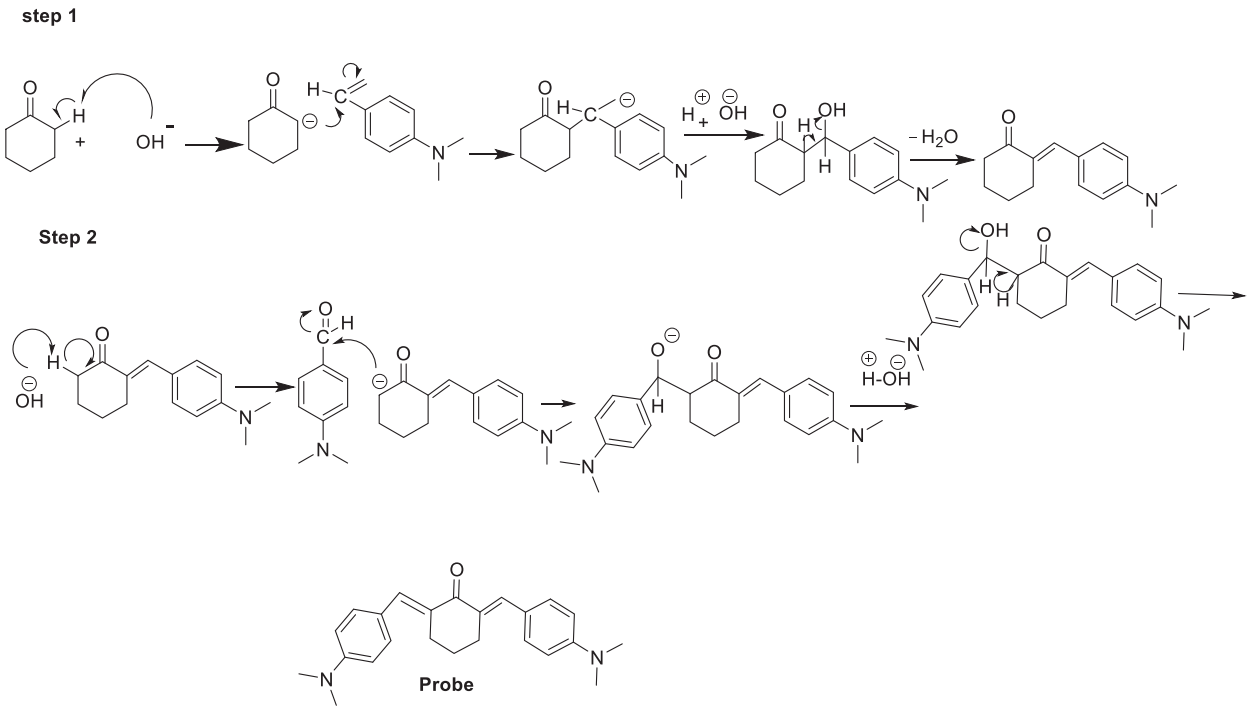

Scheme 1 Synthetic route of the probe.

Malakand, River Swat and University of Malakand, Khyber Pakhtunkhwa, Pakistan respectively in polyethylene bottles. Sufficient time was given for the settlement of solid particles in samples and then these solid residues were removed with the help of filter paper. Since Hg^{2+} ions were not found in these samples so spiking was performed to introduce ions of interest in these samples in the concentrations range of 2–12 μM. In fluorometric analysis, the concentration of probe was kept constant i.e. 6 μM. All the experiments were repeated four times in order to verify the reproducibility of the results.

2.6. Detection limit and quantification

Stern Volmer plot analysis was carried out for the detection limit and limit of quantification using the given equations

$$LOD = \frac{3\delta}{S} \tag{4}$$

$$LOQ = 3.\mathrm{LOD} \tag{5}$$

Where "δ" represent the standard deviation and "S" is the slope of the fluorescence emission intensity versus sample concentration curve. To check the repeatability of the process, respective experiment was carried out five times.

3. Results and discussion

3.1. Probe synthesis

The probe of our interest was synthesized by condensation of 4-dimethyl amino benzaldehyde with cyclohexanone by an inexpensive synthetic route (Scheme.2). The probe (yellow colored) was obtained in a significant yield as the solvent was evaporated and recrystallized in chloroform. Standard spectroscopic analyses (^{1}H NMR and FTIR) were utilized for probe confirmation.

3.2. UV–Visible studies

UV–Vis spectrum of the probe (6 μM) in acetonitrile alone and its complex with Hg^{2+} ions (15 μM) in acetonitrile distilled water mixture were taken. The probe showed λmax of 440 nm (Fig. 1a). Upon addition of Hg^{2+} solution, bathochromic shift occurred, and maximum absorption wavelength shifted to 470 nm. A regular change in absorption was observed with Hg^{2+} ion addition, at pH 7. For each measurement the baseline for probe and its complex with Hg^{2+} ions was established by placing blank acetonitrile and acetonitrile water mixture in the ratio of 3:2 in the reference compartment at 25 ± 1 °C for ligand and complex respectively.

3.3. Fluorescence measurements

The excitation and emission spectra of the probe and its complex with metal ions was recorded in 200–800 nm range. The maximum excitation and emission wavelengths were found to be 340 nm and 520 nm respectively. Hence; these wavelengths were used to carry out further fluorescence experiments. No fluorescence was observed for the blank at 520 nm. At (λex = 340 nm) and (λem = 520 nm) fluorescence emission intensity of probe linearly increases upon increase in Hg^{2+} ions in (2–18 μM) range, which is in line with UV–Vis results.

3.4. Preliminary study

The fluorescence behavior of probe (6 μM) was measured in acetonitrile at λex = 340 nm. Due to internal charge transfer phe-

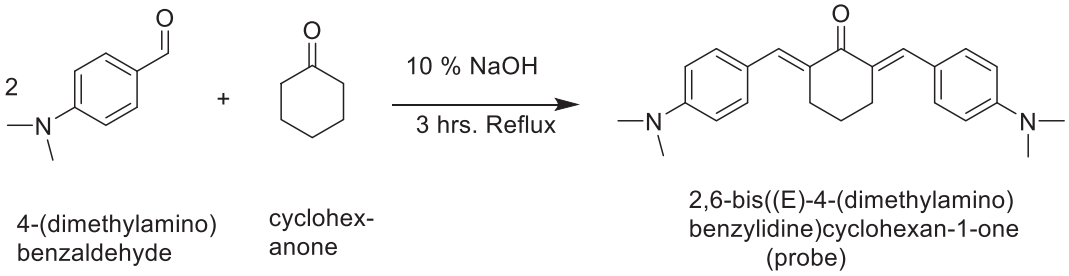

Scheme 2 Chemical structure of [(2*E*,6*E*)-2,6-bis(4-(dimethylamino)benzylidene) cyclohexanone].

nomena, very weak fluorescence was observed at λem 520 nm. To explore metal ions detection capability of probe, an equiv. of Hg^{2+} ion and 10 equiv. of different heavy and common metal ions including (Cd^{2+}, Ce^{3+}, Cr^{3+}, Zn^{2+}, Pb^{2+}, Mn^{2+}, Co^{2+}, Ni^{2+}, Cu^{2+}, Hg^{+}, Cr^{2+}, Fe^{3+}, Co^{2+}, Al^{3+}, Fe^{2+}, Mg^{2+} and Ca^{2+} were individually added to probe solution followed by equilibration of the mixture for 2 min at ambient temperature, and their fluorescence spectra recorded (Fig. 1b). Upon comparing the spectra of probe and its complex with different metal ions, the results show that fluorescence intensity enhanced largely in the presence of Hg^{2+} ions only and the rest of metal ions studied show very small enhancement. In the absence of Hg^{2+} ion, due to internal charge transfer (ICT) process, the fluorescence intensity of the probe was highly quenched. While in case of Hg^{2+} ions, ICT process is restricted, thus resulting in enhancement of fluorescence emission intensity due to formation of stable complex.

3.5. Optimization study

Different parameters were optimized for the accurate determination of Hg^{2+} ion in water samples using the probe.

3.5.1. Effect of response time on fluoresce intensity

For the real time metal ions detection in aqueous samples, the response of the probe should be very fast as the long reaction time is undesired. Therefore, the response time of probe towards Hg^{2+} ion was studied by taking probe (6 μM) and Hg^{2+} ion in the range of (2–18 μM) and varying the time of complex formation between the two from 1 to 15 min, at λem = 520 nm (Fig. 1c). The probe and its Hg^{2+} ion complex fluorescence emission response gradually increases with time, and maximum fluorescence emission intensity was observed in 2 min for lower concentration of Hg^{2+} ion, whereas for higher concentration of Hg^{2+}, probe response becomes almost instantaneous and the maximum fluorescence intensity was observed in less than 40 s time. No apparent enhancement in fluorescence emission intensity took place in the absence of metal ion in the assay time showing its stability. The spontaneous response of probe towards Hg^{2+} ion confirm its practical applicability in aqueous samples.

3.5.2. Effect of probe concentration

To investigate the effect of concentration of probe on fluorescence emission response of Hg^{2+} complex, different working solution were analyzed separately, at λem = 520 nm and the results were plotted against fluorescence emission intensity (Fig. 1d). Working solutions for analysis were prepared with addition of probe solution in the range (5–45 μM) in the presence of Hg^{2+}(15 μM). Upon increasing concentration of probe, the fluorescence emission intensity increased gradually upto (45 μM). After that, no visible enhancement in fluorescence intensity was observed. The reproducibility of the probe was determined with the help of replicate analysis. Eight replicate analyses were conducted using same concentration of Hg^{2+} and probe i.e. (15 μM) and the relative standard deviation (RSD) came out to be 0.34% (Liu and Lu, 2007).

3.5.3. Effect of mercury ions concentration on fluorescence response and detection limit

The binding ability of the probe towards Hg^{2+} ion was investigated quantitatively through fluorescence experiments. The sensitivity of probe was examined with increasing Hg^{2+} ion at room temperature. The probe showed a very weak fluorescence response at λem = 520 nm and λex at 340 nm in the absence of Hg^{2+} ion, on the other hand fluorescence response of probe (6 μM) rapidly increased on addition of Hg^{2+} ion in the range of (2–18 μM) as shown in (Fig. 2e) at the same wavelengths of excitation and emission. The linearity of the probe was also determined by plotting the fluorescence response of probe as a function of Hg^{2+} ion in the range of (2–20 nM) at λem = 520 nm. This linear response is shown in (Fig. 2f) with 0.997 R^2 value. The limit of detection of probe for Hg^{2+} ion based on five blank measurement was found to be 2.7 nM, which is far less than the acceptable value recommended by WHO (Huang et al., 2014). The limit of detection of probe reported in present work is also less than the already reported ligands/probes for mercury ion as given in (Table 1). The limit of quantification for the current probe as determined from the fluorescence experiments is found to be 3 nM based on equation (3).

3.5.4. Job's plot analysis

The binding stoichiometric ratio of probe with Hg^{2+} ion was calculated with Job's plot analysis employing fluorescence spectroscopy. The equimolar solutions of probe and Hg^{2+}ion were prepared and analysis was carried out by continuously increasing one part and decreasing another part, while total concentration of both probe and Hg^{2+} ion kept constant at (12 μM). Binding ratio was determined by plotting their respective fluorescence emission intensities at different fractions of probe (0.1 to 0.9). Maximum fluorescence emission intensity was obtained at a molar fraction of 0.7 at λem = 5 20 nm, indicating 2:1 binding ratio between probe and Hg^{2+} ion (Fig. 2g) (Sadia et al., 2018).

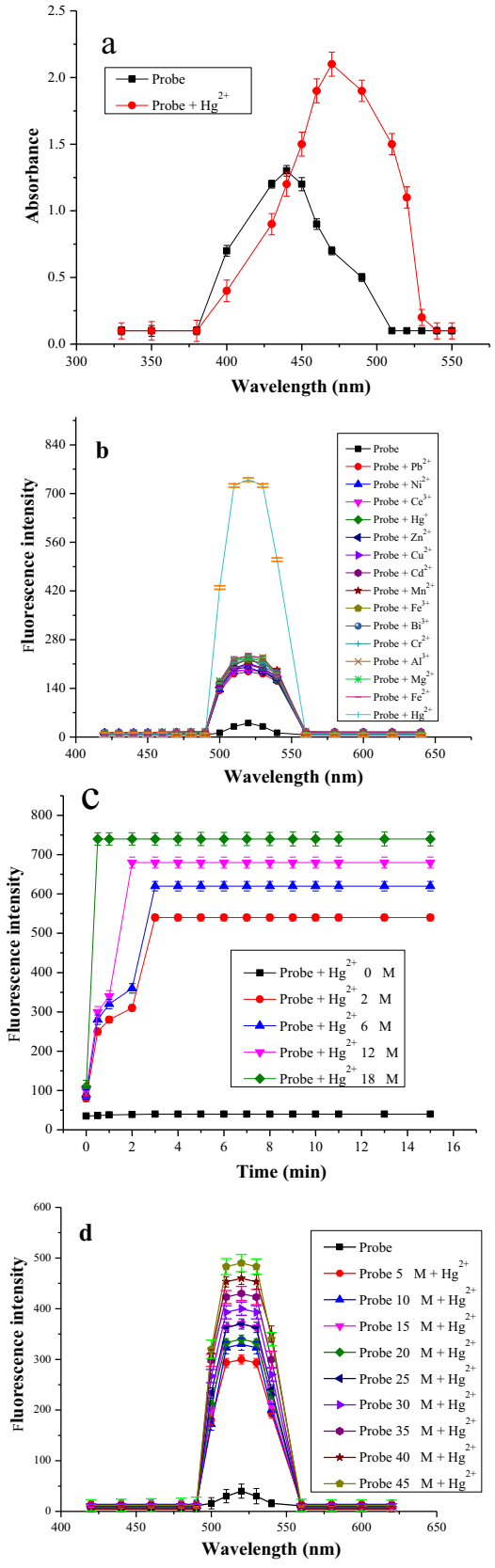

3.5.5. *Benesi–Hildebrand plot analysis for association constant determination*

Association constant value was calculated based on Benesi–Hildebrand plot from Eq. (6)

$$\frac{F_{max-}F^{\circ}}{F-F^{\circ}} = 1 + \frac{1}{Ka[Hg^{2+}]^2} \tag{6}$$

In equation Ka, "F_0", "Fmax" and "F" indicate association constant, intensity of probe without metal ion, [Hg^{2+}] in large excess and at different [Hg^{2+}] (λex = 340 nm and λem = 520 nm. The association constant Ka was determined by plotting Fmax-F∘/F-F∘ versus 1/[Hg^{2+}]^2 (Fig. 2h). According to the equation data fitted linearly showing excellent liner relationship with (7.432×10^{-11}), (1.184) slope and intercept respectively. The association constant value was calculated from the slope and intercept of the graph to be 1×10^{11} M^{-2}.

3.5.6. *Effect of pH*

In fluorometric analysis stable complexes were formed at specific pH, therefore pH optimization studies were carried out to evaluate the practical applicability of the probe. The working solution (6 μM) of probe and (12 μM) Hg^{2+} ion were prepared in acetonitrile and water respectively. NaOH and HCl were used to adjust the pH in (2–12) range. Fluorescence emission intensities of each solution was recorded at λem = 520 nm (Fig. 3(l)). The emission intensity of probe remained unaffected by changing pH. On the other hand, upon changing pH of Hg^{2+} ion complex solution, an apparent change in fluorescence response was observed due to electrons lone pairs on nitrogen and O sites. At low pH, the complex was unstable thus quenching fluorescence due to protonation of carbonyl oxygen and nitrogen. Maximum fluorescence emission intensity for the complex occurred at pH 7, indicating its high stability. At pH > 7, a drop off in fluorescence emission intensity takes place due to formation $Hg(OH)_2$, indicating that no Hg^{2+} ion complex formation occurs (Oliveira and Morais 2018,Wang et al., 2019). The results obtained reveal the applicability of probe in real life at physiological pH.

3.5.7. *Interference study*

In real samples we come across a complex matrix containing a number of other metal ions in addition to the metal of concern. Therefore the selectivity is a very important parameter in fluorigenic detection of metal of interest. Different competitive experiments were performed for evaluating selectivity and practicality of probe for Hg^{2+} ions in the presence of different metal ions which can act as interferer. The change in the fluorescence response of probe at λem = 520 nm was recorded by

Fig. 1 **a**) Absorption spectra of the probe (6 μM) and probe-Hg^{2+} mixture (15 μM) in acetonitrile and distilled water respectively **b**) Initial fluorescence study of probe (6 μM) with Hg^{2+} (15 μM) and other heavy metals (250 μM) in acetonitrile and distilled water respectively, **c**) Time course of the fluorescence response of probe (6 μM) in acetonitrile in the presence of different concentrations of Hg^{2+} (2–18 μM) in distilled water, **d**) The response of probe towards Hg^{2+} (15 μM) in distilled water with varying concentration of probe (5–45 μM) in acetonitrile.

taking the sample solution containing probe (6 μM) and a number of possible interfering metal ions like Cr^{3+}, Ce^{3+}, Cu^{2+}, Zn^{2+}, Cd^{2+}, Pb^{2+}, Mn^{2+}, Co^{2+}, Zn^{2+}, Ni^{2+}, Cr^{2+}, Li^{2+}, Al^{3+}, Fe^{2+}, Mg^{2+} and Hg^{+} (250 μM) followed by the addition of Hg^{2+} (50 μM). No significant interference was observed from the competing metal ions, thus showing that probe can be useful as an excellent sensitive, and selective fluorescence-on sensor for trace amount determination of Hg^{2+} ion with a large amount of other co-existing metal ions (Fig. 3k) (Zhu et al., 2010, Wang et al., 2020, Lee et al., 2014).

3.5.8. DFT calculations

The coordination sites present in the probe include two N and one carbonyl oxygen (Scheme. 3). The probe is probable to act as either monodentate or bidentate. In either case, the proposed structure will be afforded. The coordination sphere of d-block elements like Hg^{2+} is either 4 (Rosiaket al., 2018) or in several cases, 2 (Dong et al., 2017). Due to the bulkness of probe, the bonding is strong, consequently, to gain fully insights into the bonding strength between the active sites i.e. O and N of the probe and Hg^{2+} ion, we performed density functional theory (DFT) simulations (Fig. 3J). Now a days the DFT simulations are the powerful tool to predict correctly the bonding behaviors between the probe and Hg^{2+} ion (Lamiel-Garcia et al., 2017, Khan et al., 2019, Ahmad et al., 2002, Khan et al., 2019). The DFT simulations were performed by B3LYP level of theory and 6-31G (d,p) basis set for H, C, N and O atoms and LANL2DZ basis set for Hg^{2+} metal implemented in Gaussian-09 code (Suet al., 2017). As we proposed two sites for the binding of Hg^{2+}, site-1 is the O site (C = O group) and N site (C—$N(CH_3)_2$ group).

Therefore, we performed two different computations for the interaction of Hg^{2+} ion with the probe at two different sites i.e. O and N. As in our experiments we used 2:1 of probe and Hg^{2+} ion therefore, in computational simulations we also used 2:1 of probe and Hg^{2+} ion. The optimized geometry of probe and their complexes (Hg^{2+} binding with probe at O site and N site). The geometry optimization reveals that the Hg^{2+} ion formed a binding distance of 2.22 Å with O atom of C = O group while the binding energy (E_b) of complex is −305.69 kcal/mol in gas phase respectively. The higher negative value of binding energy shows binding of Hg^{2+} ion due to O site is energetically more preferable. Moreover, the natural atomic charges results obtained through Mullikan atomic charge analysis shows −0.057 e charge transfer occurred from the Hg^{2+} atom to the O atom which evidence stronger overlapping between the O and Hg^{2+} ion. The interaction of Hg^{2+} ion with the N site of probe, shows that the Hg^{2+} ion form a binding distance of 4.41 and 5.46 Å with the N site of probe while the energetic analysis shows that the E_b values obtained for this site is −74.80 Kcal/mol, shows weaker interactions as compared to C = O site. The atomic charge analysis indicated that there is (0.004 e) transfer occurred from the

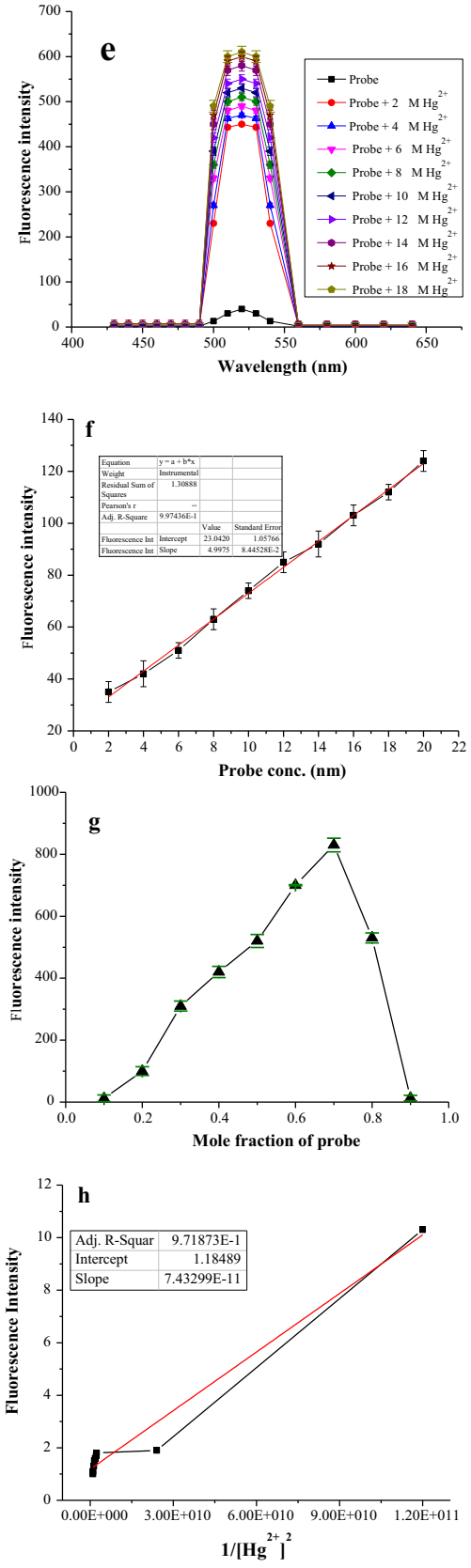

Fig. 2 **e**) Effect of Hg^{2+} ion concentration on fluorescence response of probe (6 μM) in acetonitrile with varying Hg^{2+} ion (2–18 μM) in distilled water, **f).** Titration curve of probe-Hg^{2+} complex, **g)**: Jobs plot showing 2:1 binding stoichiometric ratio, **h**): Benesi-Hilderbrand plot analysis of Hg^{2+} (2–18 μM) in distilled water with probe (6 μM) in acetonitrile.

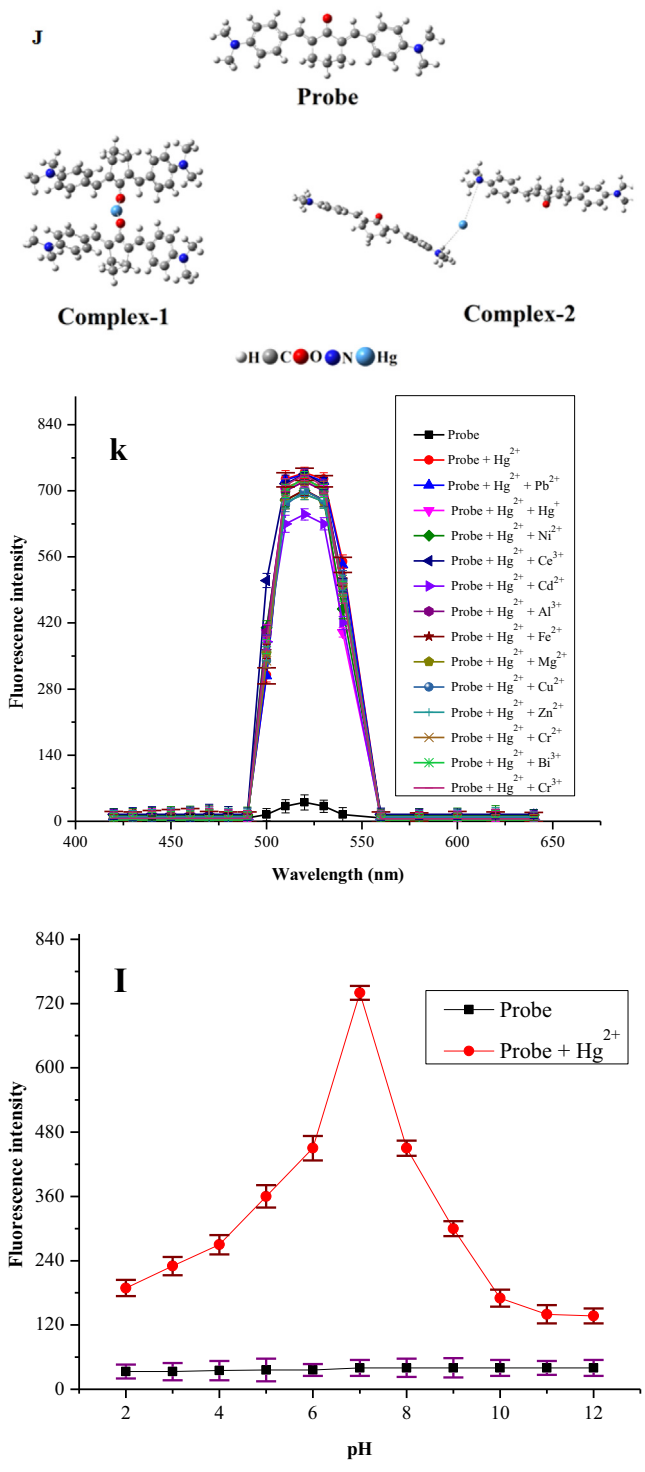

Fig. 3 **J)** Optimized geometry of synthesized probe and their complexes with Hg^{+2} ion, the binding distances are in Å, **k**). Selective response of probe (6 μM) in acetonitrile towards Hg^{2+} (50 μM) in the presence of interfering metals ions (250 μM) in distilled water at λem = 520 nm, **l).** Fluorescence response of probe (6 μM) in acetonitrile and its Hg^{2+} (12 μM) complex in distilled water as a function of pH (λex = 340 nm and λem = 520 nm).

Hg^{2+} atom to the N atoms which shows that there is no significant overlapping exist between the Hg^{2+} ion and N site of probe. The binding distances, binding energies and atomic charge analysis show that the O atom of C = O site is more reactive site for the sensing of Hg^{2+} ion. Therefore, for deep understanding of the sensing mechanism of Hg^{2+} ion through C = O site, we further investigated the thermodynamic analysis and the effect of solvent phase on the sensing phenomenon. The computation shows that the change in enthalpy (ΔH) and change in Gibbs free energy (ΔG) value calculated for the studied complex is −302.733 kcal/mol and −281.89 kcal/mol in gas phase respectively. The negative values of thermodynamic parameters evince that the sensing process is spontaneous and feasible at room temperature. The value of ΔH and ΔG for Hg^{2+} ion interaction with the C = O site of ligand in solvent phase was calculated and is −197.39 kcal/mol and −164.84 kcal/mol, respectively (Table S1).The binding energies and thermodynamic parameters values in the gas phase are higher than the solvent phase, which may be due to the strong columbic interactions between the charged-Hg(II) cations and negative C = O group without interference of other ion or molecule (Ali et al., 2020, Remko et al., 2020). Thus, the DFT results show that the synthesized probe has higher affinity for the Hg^{2+} ion sensing through its O site of C = O bond as compared to the N site of C-N$(CH_3)_2$ group. Furthermore, the results reveal that the synthesized probe have greater tendency for the sensing Hg^{2+} ion in spiked samples due to its higher binding energy and larger charge transfer.

3.5.9. ICT mechanism for Hg^{2+} ion detection

The Hg^{2+} ion detection mechanism of probe was proposed to be intra molecular charge transfer (ICT) through fluorometric analysis. Before coordination with Hg^{2+} ion, probe was found to be very weakly fluorescent due to lone pair of electrons with oxygen atom, which result in intra molecular charge transfer. Moreover, the lone electron pair of the oxygen atom give rise to a non-radiative process by the n-π* transition, as a result fluorescence emission intensity quenched. Alternatively, after coordination of probe to Hg^{2+} ion, radiation process was primarily via π-π* transitions and the coordination complex was more rigid, thus the ICT process was restricted upon addition of Hg^{2+} ion at the receptor site (Kauret al., 2018, Quang et al., 2010, Lal et al., 2020).

3.5.10. Mercury ion detection in water samples

The selectivity and sensitivity of the probe (6 μM) was validated by plotting the fluorescence response of probe as a function of increasing Hg^{2+} ion concentration (2–12 μM) in different spiked aqueous samples collected from natural sources (lake, river and tap). As natural water samples contain salts, different metal ions in high amount and has variable pH, but despite of all that, a linear response of probe (Fig. 4m) with increasing Hg^{2+} concentration was observed suggesting that the probe has the potential to monitor Hg^{2+} ions in real samples.

3.5.11. Reversibility study

Reversibility is the most important aspect in establishment of the fluorogenic probe. Reversibility plays a very important role in practical assay. The increase in the fluorescence intensity can also be due to photo activation of probe or a chemical reaction

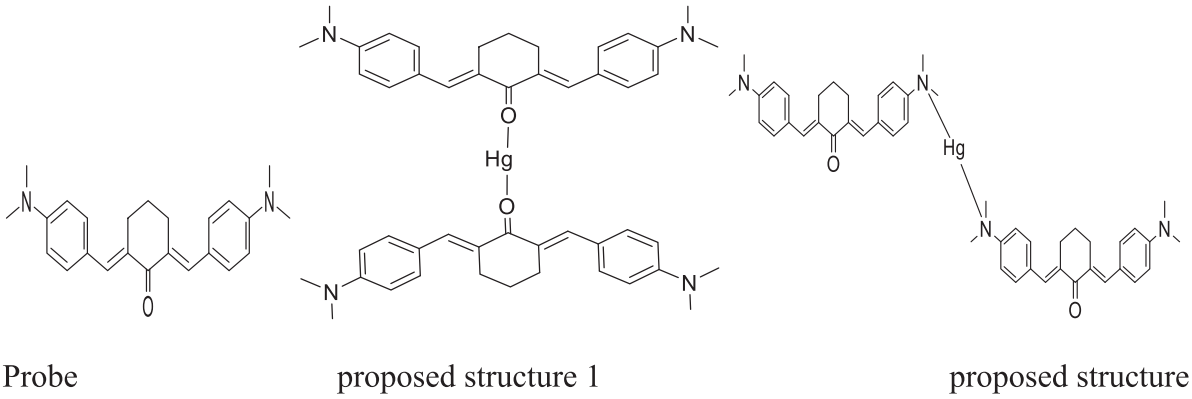

Scheme 3 Proposed structures of probe and Hg^{2+}-complex by up taking two folds of probe at optimized conditions of temperature and pH.

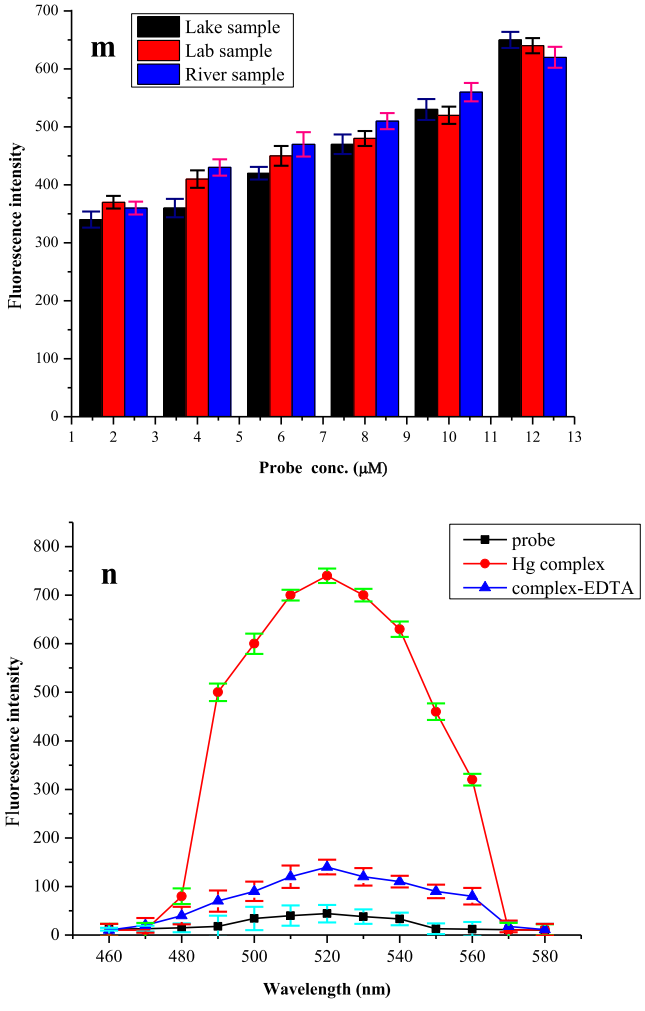

Fig. 4 **m**) Fluorometric detection of Hg^{2+} ion in spiked water samples containing Hg^{2+} ion (2–12 μM) in distilled water and probe (6 μM) in acetonitrile, **n**). Reversibility of probe (6 μM) in acetonitrile and Hg^{2+} (25 μM) by the addition of EDTA (25 μM) to the complex solution.

Table 2 List of symbols used in the manuscript.

Symbols	stands for
δ	standard deviation
S	slope
Λ	wavelength
μM	micromolar
Ka	association constant

between probe and Hg^{2+} therefore the exact cause of enhancement in fluorescent emission intensity was investigated by performing a reversibility experiment of probe (6 μM) with Hg^{2+} ion (25 μM). For this purpose, a strong chelating agent, ethylene-diamine tetra-acetic acid (EDTA) was employed to regress the fluorescence. An equal amount of ethylene-diamine tetra-acetic acid (25 μM) solution was used in Hg^{2+} complex with probe and fluorescence emission intensity was observed at λem = 520 nm (Fig. 4n). At this wavelength, the fluorescence signal was reproduced showing the chemical reversibility and real binding of Hg^{2+} ion with probe. The symbols used in the current article are presented in (Table 2).

4. Conclusion

In conclusion, a curcumin derivative (probe) was synthesized by conventional method and its structural elucidation was carried out by Proton nuclear magnetic resonance and Fourier transform infrared spectroscopic techniques. The chemically stable probe showed a fluorescence-on response for trace level detection of Hg^{2+} ion in aqueous samples, executing negligible interfering metal ions effect. The density-functional theory study supported the 2:1 binding ratio between probe and Hg^{2+} ion, as calculated by fluorescence experiments with the help of Job's plot analysis. The association constant value was calculated to be 1×10^{11} M^{-2} by Benesi-Hilderbrand plot. In addition, probe functions as a reversible fluorescence-on probe for Hg^{2+} detection in the presence of ethylenediaminetetraacetic acid as restoring agent.

CRediT authorship contribution statement

Jehangir Khan: Methodology. **Maria Sadia:** Conceptualization, Writing – review & editing. **Syed Wadood Ali Shah:** Visu-

alization. **Muhammad Zahoor:** Supervision. **Khalaf F Alsharif:** Validation. **Fakhria A. Al-Joufi:** Validation.

Declaration of Competing Interest

The authors declare that they have no known competing financial interests or personal relationships that could have appeared to influence the work reported in this paper.

Acknowledgments

This work was supported by the Taif University Researchers Supporting Program (Project number: TURSP-2020/153), Taif University, Saudi Arabia.

Funding

There has been no significant financial support for conduction of current research work that could have influenced its outcomes.

Appendix A. Supplementary material

Supplementary data to this article can be found online at https://doi.org/10.1016/j.arabjc.2022.103710.

References

Agheriand, H., Naderi, M., 2009. Immersed single-drop microextraction–electrothermal vaporization atomic absorption spectroscopy for the trace determination of mercury in water samples. J. Hazard. Mater. 165 (1–3), 353–358.

Ali, Z., Ahmad, R., Farooq, W.A., Khan, A., Khan, A.A., Bibi, S., Atif, M., 2020. Synthesis and characterization of functionalized nanosilica for zinc Ion mitigation; experimental and computational investigations. Molecules 25 (23), 5534.

Arakaki, L., Filha, V.A., Germano, A., Santos, S., Fonseca, M., Sousa, K., Espinola, J., Arakaki, T., 2013. Silica gelmodified with ethylenediamine and succinic acid–adsorption and calorimetry of cations in aqueous solution. Thermochim. Acta. 556, 34–40.

Badal, M.M.R., Ashekul, I.H.M., Maniruzzaman, M., Abu-Yousuf, M., 2020. Acidochromic behavior of dibenzylidene cyclohexanone-based bischalcone: experimental and theoretical study. ACS omega. 5 (36), 22978–22983.

Chen, L., Yang, L., Li, H., Gao, Y., Deng, D., Wu, Y., Ma, L.J., 2011. Tridentate lysine-based fluorescent sensor for Hg (II) in aqueous solution. Inorg. Chem. 50 (20), 10028–10032.

Date, Y., Aota, A., Terakado, S., Sasaki, K., Matsumoto, N., Watanabe, Y., Ohmura, N., 2013. Trace-level mercury ion (Hg2 +) analysis in aqueous sample based on solid-phase extraction followed by microfluidic immunoassay. Anal. Chem. 85 (1), 434–440.

Ding, L., Liu, Y., Zhai, J., Bond, A.M., Zhang, J., 2014. Direct electrodeposition of graphene-gold nanocomposite films for ultrasensitive voltammetric determination of mercury (II). Electroanalysis. 26 (1), 121–128.

Dong, Y., Fan, R., Chen, W., Wang, P., Yang, Y., 2017. A simple quinolone schiff-base containing CHEF based fluorescence 'turn-on'chemosensor for distinguishing Zn^{2+} and Hg^{2+} with high sensitivity, selectivity and reversibility. Dalton Trans. 46 (20), 6769–6775.

Gonzalez, R.H., Liu, G., Liriano, C., Li, Y., Yin, Y., Shi, J., Cai, Y., 2017. Elemental mercury: Its unique properties affect its behavior and fate in the environment. Environ. Pollut. 229, 69–86.

Grimme, S., 2006. Semi empirical GGA-type density functional constructed with a long-range dispersion correction. J. Comput. Chem. 27 (15), 1787–1799.

Hakimifar, A., Morsali, A., 2018. Urea-based metal–organic frameworks as high and fast adsorbent for Hg^{2+} and Pb^{2+} removal from water. Inorg. Chem. 58 (1), 180–187.

He, H., Zhu, Q.Q., Li, C.P., Du, M., 2018. Design of a highly-stable pillar-layer zinc(II) porous framework for rapid, reversible, and multi-responsive luminescent sensor in water. Cryst. Growth Des. 19 (2), 694–703.

Ho, I., Chu, J.H., Chung, W.S., 2011. Calix [4] arene with lower-rim beta-amino alpha, beta-unsaturated ketones containing bis-chelating sites as a highly selective fluorescence turn-on chemosensor for two copper (II) ions. European J. Org. Chem. 8, 1472–1481.

Huang, J., Gao, X., Jia, J., Kim, J.K., Li, Z., 2014. Graphene oxide-based amplified fluorescent biosensor for Hg^{2+} detection through hybridization chain reactions. Anal. Chem. 86 (6), 3209 3215.

Idros, N., Chu, D., 2018. Triple-indicator-based multidimensional colorimetric sensing platform for heavy metal ion detections. ACS Sens. 3 (9), 1756–1764.

JG, M. 2017. A new electrochemical sensor based on modified carbon nanotube-graphite mixture paste electrode for voltammetric determination of resorcinol. *Asian J Pharm Clin Res*, *10*(12), 295-300.

Joksimovic, D., Stankovic, S., 2012. The trace metals accumulation in marine organisms of the southeastern Adriatic coast. Montenegro. J. Serbian Chem. Soc. 77 (1), 105–117.

Kaur, B., Kaur, N., kumar, S., 2018. Colorimetric metal ion sensors-a comprehensive review of the years 2011–2016. Coord. Chem. Rev. 358, 13–69.

Khan, A.A., Esrafili, M.D., Ahmad, A., Hull, E., Ahmad, R., Jan, S. U., Ahmad, I., 2019. A computational study on the characteristics of open-shell H-bonding interaction between carbamic acid (NH_2-COOH) and HO_2, HOS or HSO radicals. J. Mol. Model. 25 (7), 189–196.

Kumar, Y., Kaushik, R., Rani, S., Rafat, S., Shabir, J., Dev, K., Kumar, L.S., 2021. Curcumin immobilized metal organic framework based fluorescent nanoprobe for selective sensing and bioimaging of Fe (II). Mater. Today Commun. 28, 102–113.

Lal, S., Prakash, K., Khera, N., Singh, S., Singh, A., Hooda, S., Chadra, R., 2020. Curcumin based supramolecular ensemble for optical detection of Cu^{2+} and Hg^{2+} ions. J. Molec. Struct. 6, 121–127.

Lamiel-Garcia, O., Ko, K.C., Lee, J.Y., Bromley, S.T., Illas, F., 2017. When Anatase nanoparticles become bulklike: Properties of realistic TiO_2 nanoparticles in the 1–6 nm size range from all electron relativistic density functional theory based calculations. J. Chem. Theory Comput. 13 (4), 85–93.

Lee, H.G., Kim, K.B., Park, G.J., Na, Y.J., Jo, H.Y., Lee, S.A., Kim, C., 2014. An anthracene-based fluorescent sensor for sequential detection of zinc and copper ions. Inorg. Chem. Commun. 39, 61–65.

Lin, L.R., Tang, H.H., Wang, Y.G., Wang, X., Fang, X.M., Ma, L.H., 2017. Functionalized lanthanide (III) complexes constructed from azobenzene derivative and β-diketone ligands: luminescent, magnetic, and reversible *trans*-to-*cis* Photoisomerization properties. Inorg. Chem. 56 (7), 3889–3900.

Liu, D., Yu, W., Li, J., Pang, C., Zhao, L., 2013. Novel 2-(E)-substituted benzylidene-6-(N-substituted aminomethyl) cyclohexanones and cyclohexanols as analgesic and anti-inflammatory agents. Med Chem Res. 22 (8), 3779–3786.

Liu, J., Lu, Y., 2007. A DNAzyme catalytic beacon sensor for paramagnetic Cu^{2+} ions in aqueous solution with high sensitivity and selectivity. J. Am. Chem. Soc. 129 (32), 9838–9839.

Liu, Y., Ouyang, Q., Li, H., Zhang, Z., Chen, Q., 2017. ACS Appl. Mater. Interfaces 9, 18314–18321.

Louie, H., Wong, C., Huang, Y.J., Fredrickson, S., 2012. A study of techniques for the preservation of mercury and other trace elements in water for analysis by inductively coupled plasma mass spectrometry (ICP-MS). Anal. Methods. 4 (2), 522–529.

Ma, X., Li, Y., Ye, Z., Yang, L., Zhou, L., Wang, L., 2011. Novel chelating resin with cyanoguanidine group: useful recyclable materials for Hg(II) removal in aqueous environment. J. Haz. Mat. 185 (2–3), 1348–1354.

Manjunatha, J.G., 2018. A novel voltammetric method for the enhanced detection of the food additive tartrazine using an electrochemical sensor. Heliyon 4, (11) e00986.

Manjunathaa, J.G., Deraman, M., Basri, N.H., Talib, I.A., 2014. Selective detection of dopamine in the presence of uric acid using polymerized phthalo blue film modified carbon paste electrode. Adv Mat Res. 895, 447–451.

Marenich, A.V., Cramer, C.J., Truhlar, D.G., Guido, C.A., Mennucci, B., Scalmani, G., Frisch, M.J., 2011. Practical computation of electronic excitation in solution: vertical excitation model. Chem. Sci. 2 (11), 2143–2161.

Marenich, A.V., Cramer, C.J., Truhlar, D.G., 2009. Universal solvation model based on solute electron density and on a continuum model of the solvent defined by the bulk dielectric constant and atomic surface tensions. J. Phys. Chem. B 113, 6378–6396.

Meenatchi, V., Muthu, K., Rajasekar, M., Meenakshisundaram, S.P., Mojumdar, S.C., 2015. Synthesis, growth, structure and characterization of (2e,6E)-2-)4-bromobenzylidine)-6-(4-methoxybenzylidine) cyclohaxanone. J. Therm. Anal. Calorim. 119 (2), 921–930.

Nehla, P., Ulrich, C., Dhaka, R.S., 2019. Investigation of the structural, electronic, transport and magnetic properties of Co_2-FeGa Heusler alloy nanoparticles. J. Alloys Compd. 776, 379–386.

Novaak, P., Deedina, J., Kratzer, J., 2016. Preconcentration and atomization of arsane in a dielectric barrier discharge with detection by atomic absorption spectrometry. *Anal*. Chem. 88 (11), 6064–6070.

Oliveira, T.M., Morais, S., 2018. New generation of electrochemical sensors based on multi-walled carbon nanotubes. Appl. Sci. 8 (10), 125–132.

Panhwar, A.H., Tuzen, M., Kazi, T.G., 2017. Ultrasonic assisted dispersive liquid-liquid microextraction method based on deep eutectic solvent for speciation, preconcentration and determination of selenium species (IV) and (VI) in water and food samples. Talanta. 175, 352–358.

Quang, D.T., Kim, J.S., 2010. Fluoro-and chromogenic chemodosimeters for heavy metal ion detection in solution and biospecimens. Chem. Rev. 110 (10), 6280–6301.

Raj, S., Shankaran, D.R., 2016. Curcumin based biocompatible nanofibers for lead ion detection. Sens. Actuators B Chem. 226, 318–325.

Razavi, A.A., Masoomi, M.Y., Morsali, A., 2017. Double solvent sensing method for improving sensitivity and accuracy of Hg(II) detection based on different signal transduction of a tetrazine-functionalized pillared metal–organic framework. Inorg. Chem. 56 (16), 9646–9652.

Richard, J.H., Bischoff, C., Ahrens, C.G., Biester, H., 2016. Mercury (II) reduction and co-precipitation of metallic mercury on hydrous ferric oxide in contaminated groundwater. Sci. Total Environ. 539, 36–44.

Rosiak, D., Okuniewski, A., Chojnacki, J., 2018. Novel complexes possessing Hg–(Cl, Br, I)$\cdots$ OC halogen bonding and unusual Hg_2S_2(Br/I)4 kernel. The usefulness of $\tau4'$ structural parameter. Polyhedron. 146, 35–41.

Sadia, M., Naz, R., Khan, J., Khan, R., 2018. Synthesis and evaluation of a schiff-based fluorescent chemosensors for the selective and sensitive detection of Cu^{2+} in aqueous media with fluorescence off-on responses. J. Fluoresc. 28 (6), 1281–1294.

Somerset, V.S., Hernandez, L.H., Iwuoha, E.I., 2011. Stripping voltammetric measurement of trace metal ions using screen-printed carbon and modified carbon paste electrodes on river water from the Eerste-Kuils River System. J. Environ. Sci. Health A. 46 (1), 17–32.

Streets, D.G., Horowitz, H.M., Jacob, D.J., Lu, Z., Levin, L., Ter, A. F., Sunderland, E.M., 2017. Total mercury released to the environment by human activities. Environ. Sci Technol. 51 (11), 5969–5977.

Su, Y., Li, H., Ma, H., Robertson, J., Nathan, A., 2017. Controlling surface termination and facet orientation in Cu_2O nanoparticles for high photocatalytic activity: a combined experimental and density functional theory study. ACS Appl. Mater. Interfaces. 9 (9), 8100–8106.

Sun, D.T., Peng, L., Reeder, W.S., Moosavi, S.M., Tiana, D., Britt, D. K., Queen, W.L., 2018. Rapid selective heavy metal removal from water by a metal–organic framework/polydopamine composite. ACS Cent. Sci. 4 (3), 349–356.

Swayamsiddha, K., Gayathri, R., Shweta, S., Meera, R., Jeevan, K.P., Nageswara, R., Jagadeesh, B., Sai, S.K., Rajesh, B., Mukesh, D., 2019. Synthesis, characterization of Diarylidenecyclohexanone derivatives as new anti-inflammatory pharmacophores exhibiting strong PGE_2 and 5-LOX inhibition. New J. Chem 43, 9012–9020.

Ullah, N., Mansha, M., Khan, I., Qurashi, B., 2018. A Nanomaterial-based optical chemical sensors for the detection of heavy metals in water: Recent advances and challenges. Trends Analyt Chem. 100, 155–166.

Van, V., Park, D., Lee, Y.C., 2018. Hydrogel applications for adsorption of contaminants in water and wastewater treatment. Environ. Sci. Pollut. Res. 25 (25), 24569–24599.

Wang, X., Zhao, H., Su, Y., Zhang, C., Feng, C., Liu, Q., Shen, J., 2019. Low-temperature preparation of mechanically robust and contamination-resistant antireflective coatings for flexible polymeric glasses via embedding of silica nanoparticles and HMDS modification. ACS Appl. Mater. Interfaces. 11 (40), 37084–37096.

Wang, Z., Zhang, Y., Yin, J., Yang, Y., Luo, H., Song, J., Wang, S., 2020. A novel camphor-based "turn-on" fluorescent probe with high specificity and sensitivity for sensing mercury (II) in aqueous medium and its bioimaging application. ACS Sustain. Chem. Eng. 8 (33), 212–222.

Wijianto, B., Ritmaleni, R., Purnomo, H., Nurrochmad, A., 2020. In silico and invitro anti-inflammatory evaluation of 2,6-bis-(33-ethoxy,4-hydroxybenzylidine)cyclohexanone,2,6-bis(3-bromo,4-methoxybenzylidine)-cyclohexanone, and 2,5-bis(3,4-dimethoxybenzylidine) cyclohexanone. J. Appl. Pharm. Sci. 10 (06), 099–106.

Xu, G., Wang, J., Si, G., Wang, M., Xue, X., Wu, B., Zhou, S., 2016. A novel highly selective chemosensor based on curcumin for detection of Cu^{2+} and its application for bioimaging. Sens. Actuators B Chem. 230, 684–689.

Zhao, J., Huang, M., Zhang, L., Zou, M., Chen, D., Huang, Y., Zhao, S., 2017. Unique approach to develop carbon dot-based nanohybrid near-infrared ratiometric fluorescent sensor for the detection of mercury ions. Anal. Chem. 89 (15), 8044–8049.

Zheng, A., Chen, J., Wu, G., Wei, H., He, C., Kai, X., Chen, Y., 2009. Optimization of a sensitive method for the "switch-on" determination of mercury (II) in waters using Rhodamine B capped gold nanoparticles as a fluorescence sensor. Microchimica Acta 164 (1), 17–27.

Zhiquan, L., Niklas, P., Klaus, C., Jan, T., Samuel, C., Ligon, A., Wolfgang, H., 2013. A straightforward synthesis and strucrure activity relationship of highly efficient initiators for two photon polymerization. Macromolecules. 46 (2), 352–361.

Zhu, J.F., Yuan, H., Chan, W.H., Lee, A.W., 2010. A colorimetric and fluorescent turn-on chemosensor operative in aqueous media for Zn^{2+} based on a multi functionalized spirobenzopyran derivative. Org. Biomol. Chem. 8 (17), 3957–3964.